East Asian Journal on Applied Mathematics
doi: 10.4208/eajam.150216.260117a

Vol. 7, No. 2, pp. 325-342
May 2017

Estimation of a Regularisation Parameter for a Robin Inverse Problem

Xi-Ming Fang[1,2], Fu-Rong Lin[1] and Chao Wang[1,*]

[1] *Department of Mathematics, Shantou University, Shantou Guangdong 515063, China.*
[2] *School of Mathematics and Statistic, Zhaoqing University, Zhaoqing Guangdong 526061, China.*

Received 15 February 2016; Accepted (in revised version) 26 January 2017.

Abstract. We consider the nonlinear and ill-posed inverse problem where the Robin coefficient in the Laplace equation is to be estimated using the measured data from the accessible part of the boundary. Two regularisation methods are considered — viz. L_2 and H^1 regularisation. The regularised problem is transformed to a nonlinear least squares problem; and a suitable regularisation parameter is chosen via the normalised cumulative periodogram (NCP) curve of the residual vector under the assumption of white noise, where information on the noise level is not required. Numerical results show that the proposed method is efficient and competitive.

AMS subject classifications: 65F22, 65R32

Key words: Robin inverse problem, L_2 regularisation, H^1 regularisation, normalised cumulative periodogram (NCP) method.

1. Introduction

We consider the Robin boundary value problem for the Laplace equation in a connected open domain $\Omega \subset R^2$:

$$\begin{cases} \Delta u = 0 & \text{in} \quad \Omega, \\ \frac{\partial u}{\partial \nu} + pu = g & \text{on} \quad \partial\Omega = \Gamma, \end{cases} \tag{1.1}$$

where Γ is the boundary of the domain Ω, ν is the unit outward normal direction on Γ, g is a given current input, and p is the Robin coefficient that is nonnegative and vanishes outside $\Gamma_1 \subset \Gamma$. The Robin inverse problem is to recover the Robin coefficient p by using the data $u_0 = u|_{\Gamma_0}$ where $\Gamma_0 \subset \Gamma$ and $\Gamma_0 \cap \Gamma_1 = \phi$. This problem arises in various nondestructive detection and thermal imaging investigations [1, 16], where an unknown material profile in a non-accessible part of the boundary Γ_1 is to be recovered from a partial boundary measurement made on an accessible part of the boundary Γ_0.

*Corresponding author. *Email address:* chaowang.hk@gmail.com (C. Wang)

In the last two decades, there has been considerable progress on numerical methods for the Robin inverse problem — cf. [3, 4, 10–12, 16–18, 20, 22, 23] and references therein. In order to recover the Robin coefficient numerically, we may either express p as a linear combination of certain basis functions [2, 3] or discretise the problem [10, 19]. One can discretise (1.1) directly using finite differences or finite elements (e.g. see Ref. [19]), or reformulate it as a boundary integral equation problem that is then discretised using the boundary element method or numerical quadratures (e.g. see Refs. [17, 22]). Indeed, since both the measured data u_0 and the unknown coefficient p are on the boundary Γ, it is natural to adopt boundary integral equation approach for the Robin inverse problem (e.g. see Refs. [5, 6, 8, 10, 22]). In particular, Fasino & Inglese [11, 12, 16] proposed efficient methods for the problem in the case where $\Omega = [0,1] \times [0,a]$, $\Gamma_1 = [0,1] \times \{a\}$, and $\Gamma_0 = [0,1] \times \{0\}$ by using a "thin-plate approximation"; Lin & Fang [22] proposed an efficient quadratic programming (QP) method, in which the nonlinear Robin inverse problem is transformed to a linear problem by introducing a new variable; Jin [17] transformed the problem into an optimisation problem, and then introduced two regularisation methods in conjunction with conjugate gradient (CG) methods; and Ma & Lin [23] proposed another CG method in the setting of the boundary integral equation and introduced a functional of p as a regularisation term. Here we further consider obtaining a regularisation parameter in the boundary integral equation setting for the problem (1.1), using measured data from the accessible part of the boundary.

The regularised problem may be represented in discrete form as a nonlinear least squares problem:

$$\min_{\mathbf{p}} \frac{1}{2} \left\| R(\mathbf{p}) \right\|_2^2 + \frac{\mu}{2} \|W\mathbf{p}\|_2^2, \tag{1.2}$$

where $R(\mathbf{p})$ is the nonlinear function of $\mathbf{p}$ corresponding to the problem (1.1), W is a matrix corresponding to the regularisation method used, and $\mu > 0$ is a regularisation parameter. It is well known that the selection of a suitable value for the regularisation parameter μ is challenging, especially in the nonlinear context. Even for the linear case, there are many ways proposed in the literature — e.g. the discrepancy principle, the L-curve, the generalised cross-validation (GCV) and the normalised cumulative periodogram (NCP) curve. The discrepancy principle is based on the idea that the norm of the residual vector should be close to the norm of the noise in the measured data, which is known a priori [25]. The L-curve method plots the logarithm of the norm of the regularised solution against the squared norm of the corresponding residual for a range of values of the regularisation parameter, to choose the parameter value corresponding to the corner of the curve [15]. This is based on the fact that both the norms of the corresponding residual and the solution are functions of the regularisation parameter and that the norms have a special relation yielding the L-curve, with the parameter selected by seeking a point where the curvature is maximised. The NCP method gives the parameter value by checking if the corresponding residual vector is dominated by white noise [14]; and the GCV approach chooses the regularisation parameter by minimising the GCV function, which does not require any prior knowledge about the variance in the data [13].

In Section 2, we introduce a boundary integral equation approach to handle the Robin inverse problem, including regularisation methods. We introduce a penalty term defined by p to obtain an approximation of the Robin coefficient p, rather than a functional of both p and u as in Ref. [22], and use L_2 and H^1 regularisation methods that are very efficient in recovering continuous profiles. We introduce a Gauss-Newton method to solve the nonlinear least squares problem (1.2) for fixed parameter μ. In Section 3, we propose a parameter choice method based on the NCP curve of the residual vector. Numerical experiments in Section 4 show that the proposed algorithm can produce a near optimal regularisation parameter value, and brief concluding remarks are presented in Section 5.

2. Boundary Integral Equation Approach

As in Ref. [23], we reformulate the Robin inverse problem as a minimisation problem that only involves boundary integrals. Assume that the domain Ω has a smooth boundary Γ, the closed subsets Γ_0 and Γ_1 are disjoint, and $p(x)$ is a nonnegative function on Γ with $\mathrm{supp}(p) \subset \Gamma_1$. We have

$$\phi(x,y) = \frac{1}{2\pi} \ln \frac{1}{|x-y|}, \qquad x, y \in \Omega,\ x \neq y\,,$$

as the fundamental solution for the Laplacian equation $\triangle u = 0$ with $|x-y|$ denoting the distance between x and y. Given $p(x)$ and $g(x)$, one can obtain the function values of u on Γ by solving the following boundary integral equation

$$\frac{1}{2}u(x) + \int_\Gamma \left(\frac{\partial \phi(x,y)}{\partial \nu_y} + p(y)\phi(x,y) \right) u(y) ds_y = \int_\Gamma \phi(x,y) g(y) ds_y\,, \quad x \in \Gamma\,, \quad (2.1)$$

where ds_y denotes the differential of arc length [21]. Define

$$(\mathscr{D}u)(x) = \int_\Gamma \frac{\partial \phi(x,y)}{\partial \nu_y} u(y) ds_y \quad \text{and} \quad (\mathscr{S}u)(x) = \int_\Gamma \phi(x,y) u(y) ds_y\,, \quad x \in \Gamma\,.$$

and let

$$\mathscr{A}(p)(u) = \left(\frac{1}{2}\mathscr{I} + \mathscr{D} \right) u + \mathscr{S}(pu), \quad f = \mathscr{S} g\,,$$

so Eq. (2.1) can be written as

$$\mathscr{A}(p)(u) = f\,. \quad (2.2)$$

If the restriction operator from Γ to Γ_0 is denoted by by $\mathscr{R}_0$ (i.e. $\mathscr{R}_0 u = u|_{\Gamma_0}$), the Robin inverse problem is then to seek p such that

$$\mathscr{A}(p)(u) = f\,, \quad \mathscr{R}_0 u = u_0\,, \quad (2.3)$$

where u_0 is the measured data for u on Γ_0.

Since the Robin inverse problem is ill-posed and there is noise in u_0, a regularisation term is imposed to obtain a reasonable approximate solution. Consequently, we proceed to solve a regularised minimisation problem:

$$\min_{p,u} \frac{1}{2}\left\|\mathscr{R}_0 u - u_0\right\|^2_{L^2(\Gamma_0)} + \frac{\mu}{2}J(p) \quad s.t. \quad \mathscr{A}(p)(u) = f\,,$$

where $J(p)$ is a regularisation functional for p and $\mu > 0$ is a parameter. Thus representing u by $u = \mathscr{A}(p)^{-1}f$, we transform the problem (2.3) to the unconstrained minimisation problem

$$\min_{p} \frac{1}{2}\left\|\mathscr{R}_0\mathscr{A}(p)^{-1}f - u_0\right\|^2_2 + \frac{\mu}{2}J(p)\,. \tag{2.4}$$

As previously mentioned, we use L_2 and H^1 regularisation methods such that either

$$J(p) = J_L(p) := \int_{\Gamma_1} \left|p(x)\right|^2 ds_x \quad \text{or} \quad J(p) = J_H(p) := \int_{\Gamma_1} \left|\frac{\partial p(x)}{\partial \gamma}\right|^2 ds_x\,,$$

where γ is the normal tangent direction and ds_x is the differential of the arc length.

2.1. Discretisation

We suppose the boundary Γ is smooth and has the parametrisation

$$(x_1, x_2) = \big(\phi(t), \psi(t)\big) \quad \text{for} \quad 0 \le t \le l \quad \text{with} \quad \big(\phi(0), \psi(0)\big) = \big(\phi(l), \psi(l)\big)\,,$$

where $\phi(\cdot)$ and $\psi(\cdot)$ are both C^2 functions. Writing $u(s) = u(\phi(s), \psi(s))$, we have

$$(\mathscr{S}u)(t) = \int_0^l K_s(t,s)u(s)ds \quad \text{and} \quad (\mathscr{D}u)(t) = \int_0^l K_d(t,s)u(s)\,ds\,,$$

where

$$K_s(t,s) = -\frac{1}{2\pi}\left(\ln\sqrt{(\phi(t)-\phi(s))^2 + (\psi(t)-\psi(s))^2}\right)\sqrt{(\phi'(s))^2 + (\psi'(s))^2}\,,$$
$$K_d(t,s) = \frac{1}{2\pi}\frac{\psi'(s)(\phi(t)-\phi(s)) - \phi'(s)(\psi(t)-\psi(s))}{(\phi(t)-\phi(s))^2 + (\psi(t)-\psi(s))^2}\,.$$

We partition the interval $[0,l]$ into n uniform subintervals of length $h = l/n$. Thus let $t_i = (i-1/2)h$, $i = 1,2,\cdots,n$, and suppose

$$\{t_1, t_2, \cdots, t_n\} \cap \big\{t : (\phi(t), \psi(t)) \in \Gamma_1\big\} = \{t_{m_3+1}, \cdots, t_{m_4}\}\,,$$

so the discretisation function of $p(t)$ on Γ_1 is

$$\mathbf{p} = \big[p(t_{m_3+1}), \cdots, p(t_{m_4})\big]^{\mathrm{T}}.$$

The integral operators $\mathscr{S}$ and $\mathscr{D}$ are discretised by mid-point quadrature, and their matrix representations are denoted by D and S, respectively. If $\hat{\mathbf{p}} = (\mathbf{0}_{m_3}^T, \mathbf{p}^T, \mathbf{0}_{n-m_4}^T)^T$ where $\mathbf{0}_m$ is the zero column of length m, then we have the matrix representation of $\mathscr{A}(p)$ in (2.2):

$$A(\mathbf{p}) := \frac{1}{2}I + D + S\mathrm{diag}(\hat{\mathbf{p}}),$$

with I is the identity matrix of order n and $\mathrm{diag}(\hat{\mathbf{p}})$ the diagonal matrix generated by $\hat{\mathbf{p}}$.

We approximate the L_2 regularisation term $J_L(p)$ by

$$J_L(\mathbf{p}) = \|\mathbf{p}\|_2^2,$$

and the H^1 regularisation term $J_H(p)$ by

$$J_H(\mathbf{p}) = \sum_{i=m_3}^{m_4} (\hat{p}_{i+1} - \hat{p}_i)^2 = p_1^2 + \sum_{i=1}^{m_4-m_3-1} (p_{i+1} - p_i)^2 + p_{m_4-m_3}^2$$

on noting that $\hat{p}_{m_3} = \hat{p}_{m_4+1} = 0$, so

$$J_H(\mathbf{p}) = \|L\mathbf{p}\|_2^2$$

where

$$L = \begin{pmatrix} 1 & 0 & \cdots & 0 \\ -1 & 1 & \cdots & 0 \\ \vdots & \vdots & \ddots & \vdots \\ 0 & 0 & \cdots & 1 \\ 0 & 0 & \cdots & -1 \end{pmatrix}_{(m_4-m_3+1)\times(m_4-m_3)} . \tag{2.5}$$

Let us denote the respective discretisations of $u(t)$ and $g(t)$ on Γ by

$$\mathbf{u} = \left[u(t_1), u(t_2), \cdots, u(t_n)\right]^{\mathrm{T}}, \quad \text{and} \quad \mathbf{g} = \left[g(t_1), g(t_2), \cdots, g(t_n)\right]^{\mathrm{T}},$$

and also suppose that $\{t_1, t_2, \cdots, t_n\} \cap \{t : (\phi(t), \psi(t)) \in \Gamma_0\} = \{t_{m_1+1}, \cdots, t_{m_2}\}$ and let $\mathbf{u}_0 = [u_{m_1+1}, \cdots, u_{m_2}]^{\mathrm{T}}$. The discretisation form of (2.4) is thus

$$\min_{\mathbf{p}} F(\mathbf{p}) := \frac{1}{2}\left\|R_0 A(\mathbf{p})^{-1}\mathbf{f} - \mathbf{u}_0\right\|_2^2 + \frac{\mu}{2}\|W\mathbf{p}\|_2^2, \tag{2.6}$$

where $\mathbf{f} = S\mathbf{g}$, $R_0 = [O_{(m_2-m_1)\times m_1}\ I_{m_2-m_1}\ O_{(m_2-m_1)\times(n-m_2)}]$ with $O_{r\times s}$ being an $r \times s$ matrix of zeros, and W equals to the identity matrix of order $(m_4 - m_3)$ or L defined by (2.5).

2.2. Gauss-Newton method

We solve the minimisation problem (2.6) by the Gauss-Newton (GN) method, as it is efficient for solving nonlinear least squares problems [9]. The objective function of (2.6) can be written as

$$F(\mathbf{p}) = \frac{1}{2}\left\|\begin{pmatrix} R_0 A(\mathbf{p})^{-1}\mathbf{f} - \mathbf{u}_0 \\ \sqrt{\mu}W\mathbf{p} \end{pmatrix}\right\|_2^2,$$

and it is not difficult to get the gradient of $F(\mathbf{p})$ and the approximate Hessian matrix requited — viz.

$$\nabla F(\mathbf{p}) = -G(\mathbf{p})^{\mathrm{T}} R_0^{\mathrm{T}}(R_0\mathbf{u_p} - \mathbf{u_0}) + \mu W^{\mathrm{T}} W\mathbf{p}\,, \tag{2.7}$$

$$H(\mathbf{p}) = G(\mathbf{p})^{\mathrm{T}} R_0^{\mathrm{T}} R_0 G(\mathbf{p}) + \mu W^{\mathrm{T}} W\,, \tag{2.8}$$

where

$$\mathbf{u_p} = A(\mathbf{p})^{-1}\mathbf{f}, \qquad G(\mathbf{p}) = A(\mathbf{p})^{-1} S R_1^{\mathrm{T}} \mathrm{diag}(R_1\mathbf{u_p})$$

with $R_1 = [O_{(m_4-m_3)\times m_3}\ I_{m_4-m_3}\ O_{(m_4-m_3)\times(n-m_4)}]$.

The steps of the GN method are summarised in Algorithm 2.1.

Algorithm 2.1 Gauss-Newton method for solving (2.6).

1: Input a tolerance $\epsilon > 0$ and an initial guess $\mathbf{p}_0$. Set $k = 0$.
2: **repeat**
3: Compute $\nabla F(\mathbf{p}_k)$ and $H(\mathbf{p}_k)$ from Eqs. (2.7) and (2.8) for the current $\mathbf{p}_k$.
4: Solve $H(\mathbf{p}_k)\mathbf{d} = -\nabla F(\mathbf{p}_k)$ and compute the step length $\alpha_k = \beta^{m_k}$, where m_k is the smallest nonnegative integer m that satisfies the Armijo condition ($\beta \in (0,1), \sigma \in (0, 0.5)$):

$$F(\mathbf{p}_k + \beta^m \mathbf{d}) \le F(\mathbf{p}_k) + \sigma\beta^m \cdot \nabla F(\mathbf{p}_k)^{\mathrm{T}}\mathbf{d}\,.$$

5: Set $\mathbf{p}_{k+1} = \mathbf{p}_k + \alpha_k\mathbf{d}$ and replace k by $k+1$.
6: **until** norm$(\nabla F(\mathbf{p}_k)) < \epsilon$.

Remark 2.1. The sequence $\{\mathbf{p}_k\}$ generated by Algorithm 2.1 satisfies

$$F(\mathbf{p}_{k+1}) \le F(\mathbf{p}_k), \quad k = 0, 1, 2, \cdots.$$

Moreover, since $W^{\mathrm{T}}W$ is a positive definite matrix, the level set

$$\mathscr{L}(\mathbf{p}_0) := \{\mathbf{p} | F(\mathbf{p}) \le F(\mathbf{p}_0)\}$$

is closed and bounded — i.e. $\mathscr{L}(\mathbf{p}_0)$ is a compact subset of $\mathbb{R}^{m_4-m_3}$. Consequently, there exists a subsequence of $\{\mathbf{p}_k\}$ that converges to some point $\mathbf{p}^* \in \mathbb{R}^{m_4-m_3}$, which can be used as an approximate Robin coefficient.

3. Estimation of the Regularisation Parameter

In order to obtain a reasonable approximate Robin coefficient, a suitable value for the regularisation parameter μ should be chosen. As mentioned in Section 1, there are many methods to do so. In this section, we propose a parameter selecting method by observing that the residual vector is dominated by the remaining signal (low frequency signal) if the parameter is too large, while it is dominated by high frequency noise if the parameter is too small. Thus we start with a large μ such that the residual vector looks like low

frequency noise, and then adjust the value of μ until the corresponding residual vector looks like white noise. (Recall that white noise corresponds to a zero-mean random vector with uncorrelated elements that have the same standard deviation.)

We apply the normalised cumulative periodogram (NCP) curve of the residual vector to estimate the regularisation parameter, as first proposed in Ref. [14] — cf. also Refs. [7, 24, 26]. If the solution of (2.6) corresponding to the parameter μ is denoted by $\mathbf{p}_\mu$, then the residual vector corresponding to the fit-to-data term is

$$\mathbf{r}_\mu := R_0 A(\mathbf{p}_\mu)^{-1}\mathbf{f} - \mathbf{u}_0 \,.$$

If the discrete Fourier transform of the residual vector $\mathbf{r}_\mu$ is denoted by

$$\widehat{\mathbf{r}}_\mu = \big((\widehat{r}_\mu)_1, (\widehat{r}_\mu)_2, \cdots, (\widehat{r}_\mu)_{m_2-m_1}\big)^{\mathrm{T}} \,,$$

then the power spectrum of $\mathbf{r}_\mu$ is given by

$$\mathbf{e}_\mu = \big(|(\widehat{r}_\mu)_1|^2, |(\widehat{r}_\mu)_2|^2, \cdots, |(\widehat{r}_\mu)_{q+1}|^2\big)^{\mathrm{T}} \,,$$

where $q = \lfloor (m_2 - m_1)/2 \rfloor$ and $\lfloor a \rfloor$ denotes the maximum integer that is not larger than a. The NCP vector for the residual vector $\mathbf{r}_\mu$ is then defined as the vector $\mathrm{ncp}(\mathbf{r}_\mu)$ of length q with elements given by

$$\mathrm{ncp}(\mathbf{r}_\mu)_k = \frac{\sum_{i=2}^{k+1}(\mathbf{e}_\mu)_i}{\sum_{i=2}^{q+1}(\mathbf{e}_\mu)_i} \,, \quad k = 1, 2, \cdots, q \,.$$

Note that the first component $(\mathbf{e}_\mu)_1$ is not involved in the definition of the NCP due to the constant signal (the zeroth frequency) it represents. The curve depicted by the points $(k, \mathrm{ncp}(\mathbf{r}_\mu)_k)$, $k = 1, 2, \cdots, q$, is called the NCP curve of $\mathbf{r}_\mu$.

For a signal $\mathbf{x}$ containing only white noise, the expected power spectrum is flat and the points $(k, \mathrm{ncp}(\mathbf{x})_k)$, $k = 1, 2, \cdots, q$, lie on the line segment between the two points $(0, 0)$ and $(q, 1)$ called the ideal NCP curve — i.e. $\mathrm{ncp}(\mathbf{x})_k = k/q$, $k = 1, \cdots, q$. We denote the vector $(1/q, 2/q, \cdots, q/q)^{\mathrm{T}}$ by $\mathbf{v}$ and call it the ideal NCP vector. In brief, our aim is to choose a regularisation parameter μ such that the NCP curve of $\mathbf{r}_\mu$ is close to the ideal NCP curve. One way is to construct two lines parallel to $\mathbf{v}$ called the Kolmogorov-Smirnov (KS) limits, and then choose a parameter such that the corresponding NCP curve lies between the KS limits [14, 26] — cf. Fig. 1. When the significance level is set to 5%, the KS limits are $\pm 1.36 q^{-1/2}$ — i.e. a band of width $\pm 1.36 q^{-1/2}$ around $\mathbf{v}$ contains the NCP curve with probability 95%. A more accurate way is to choose a value of the parameter such that the corresponding NCP vector is the minimiser of $\|\mathbf{v} - \mathrm{ncp}(\mathbf{r}_\mu)\|_1$ as in Ref. [14], but that is very expensive since the objective function is not differentiable.

We propose a practical way to choose a μ value such that $\mathrm{ncp}(\mathbf{r}_\mu)$ is an approximate minimal point of $\|\mathbf{v} - \mathrm{ncp}(\mathbf{r}_\mu)\|_1$. We observe that when the regularisation parameter is large the corresponding residual vector looks like a low frequency noise, such that the NCP curve is above the ideal NCP curve since $\mathrm{ncp}(\mathbf{r}_\mu)_k$ is larger than v_k when k is small. On

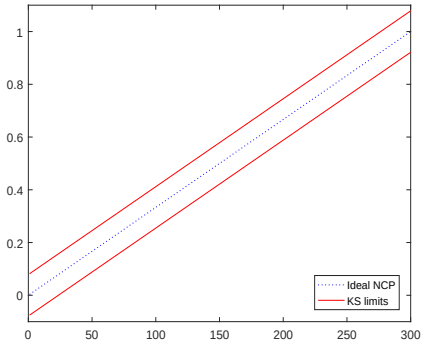

Figure 1: Ideal NCP curve and KS limits.

the other hand, if the regularisation parameter is too small, the corresponding NCP curve is below the ideal NCP curve. This can be described by the compact area between the NCP curve and x-axis — where a large parameter leads to a large area and a small one a small area via the sum of the elements of the NCP vector, and the sum corresponding to a suitable parameter μ is close to that of the ideal NCP vector. On noting that $v_k = k/q$, it is readily seen that the sum of the ideal NCP vector is

$$N_* := \sum_{k=1}^{q} k/q = (q+1)/2\,.$$

In order to seek a value μ such that

$$N(\mu) := \sum_{k=1}^{q} \mathrm{ncp}(\mathbf{r}_\mu)_k$$

is close to N_*, we start with an interval $[\mu_1,\ \mu_2]$ such that $N(\mu_1) < N_*$ and $N(\mu_2) > N_*$. Then we set the geometric mean μ_g of μ_1 and μ_2 as a regularisation parameter, and solve the minimisation problem (2.6) with the parameter $\mu_g = \sqrt{\mu_1\mu_2}$ and compute $N(\mu_g)$. We then update the interval $[\mu_1, \mu_2]$ as

$$[\mu_1', \mu_2'] = \begin{cases} [\mu_g, \mu_2], & \text{if } N(\mu_g) < N_*\,, \\ [\mu_1, \mu_g], & \text{otherwise}\,, \end{cases}$$

choose a new parameter $\mu_g' = \sqrt{\mu_1'\mu_2'}$, and solve the minimisation problem (2.6) with parameter μ_g'. To solve this efficiently, we use $\mathbf{p}_{\mu_g}$ as the initial guess. We note that $N(\mu_1') < N_*$ and $N(\mu_2') > N_*$ still hold, and the interval $[\mu_1', \mu_2']$ is smaller than $[\mu_1, \mu_2]$. The above step is then repeated until $(\mu_2 - \mu_1)/\mu_2$ is sufficiently small.

Let μ be the parameter chosen via the above procedure, and let C_μ be the NCP curve corresponding to μ. To ensure that μ is a suitable choice, we check the difference between C_μ and the ideal NCP curve by computing

$$d_\mu := \max_{k=1,\cdots,q} \left\{ |\mathrm{ncp}(\mathbf{r}_\mu)_k - v_k| \right\} \tag{3.1}$$

and using the KS limits. If d_μ is smaller than $1.36q^{-1/2}$, then the NCP curve C_μ is close to the ideal one, which means that μ is suitable. If d_μ is larger than $1.36q^{-1/2}$, then μ is too small, and we need to adjust the initial interval.

The procedure can be summarised as Algorithm 3.1.

Algorithm 3.1 Choice of regularisation parameter.

1: Input initial values $\mathbf{p} = \mathbf{p}_0$ and $[\mu_1,\ \mu_2]$.
2: **repeat**
3: Set $\mu_g = \sqrt{\mu_1\mu_2}$.
4: Solve the minimisation problem (2.6) with parameter μ_g.
5: Compute $N(\mu_g) = \sum \mathrm{ncp}(\mathbf{r}_{\mu_g})$, where $\mathbf{r}_{\mu_g}$ is the residual vector.
6: If $N(\mu_g) < N_*$, set $\mu_1 = \mu_g$, otherwise set $\mu_2 = \mu_g$.
7: **until** $(\mu_2 - \mu_1)/\mu_2$ is sufficiently small.
8: Compute $\mathbf{p} = \max\{\mathbf{p}_{\mu_g}, 0\}$ (replace the negative components of $\mathbf{p}_{\mu_g}$ by zero), where $\mathbf{p}_{\mu_g}$ is the result of the final step.
9: Compute d_μ using (3.1). If $d_\mu \geq 1.36q^{-1/2}$, then adjust the initial interval $[\mu_1,\ \mu_2]$ and go to Step 2.

To end this section, we remark on how best to choose $[\mu_1,\ \mu_2]$. We first solve (2.6) with a large μ so the minimisation problem (2.6) can be solved readily, and compute $N(\mu)$. If $N(\mu) > N_*$, set $\mu' = t\mu$, but otherwise set $\mu' = \mu/t$ where $t < 1$ (say, $t = 0.1$) is a compression factor. Consider the case where $N(\mu) > N_*$ (the case $N(\mu) < N_*$ can be handled similarly). If $N(\mu') < N_*$, set $[\mu_1, \mu_2] = [\mu', \mu]$. Otherwise, replace μ by μ' and μ' by $t\mu'$, respectively. Repeat the procedure until $N(\mu') < N_*$ and set $[\mu_1, \mu_2] = [\mu', \mu]$.

Our numerical tests show that if we choose the initial interval as above and seek μ by using Algorithm 3.1, then the adjustment step is not required. Our numerical tests also show that if μ is very small then it is possible that $N(\mu)$ is close to N_* while C_μ is not close to the ideal NCP curve, since C_μ can be '$\curlywedge$'-shaped. In this case, we can see that $\mathbf{r}_\mu$ is dominated by high frequency components, which indicates that the regularisation parameter μ is too small and we need to choose a larger regularisation parameter.

4. Numerical Examples

In this section, we present numerical results to illustrate the effectiveness of the proposed methods. We chose an example that has been tested in the literature — cf. [22, 23]. Thus we considered Eq. (1.1) in an elliptic domain $x_1^2/a^2 + x_2^2/b^2 \leq 1$ where $a = 1$ and $b = 0.1$, with the usual parametrisation of its elliptical boundary $\Gamma : x_1^2/a^2 + x_2^2/b^2 = 1$:

$$x = x(t) = \big(a\cos(2\pi t), b\sin(2\pi t)\big), \quad 0 \leq t \leq 1\,.$$

The two segments Γ_0 and Γ_1 chosen were

$$\Gamma_0 = \big\{(a\cos(2\pi t), b\sin(2\pi t)) : t \in [0.55, 0.85]\big\},$$
$$\Gamma_1 = \big\{(a\cos(2\pi t), b\sin(2\pi t)) : t \in [0.15, 0.45]\big\},$$

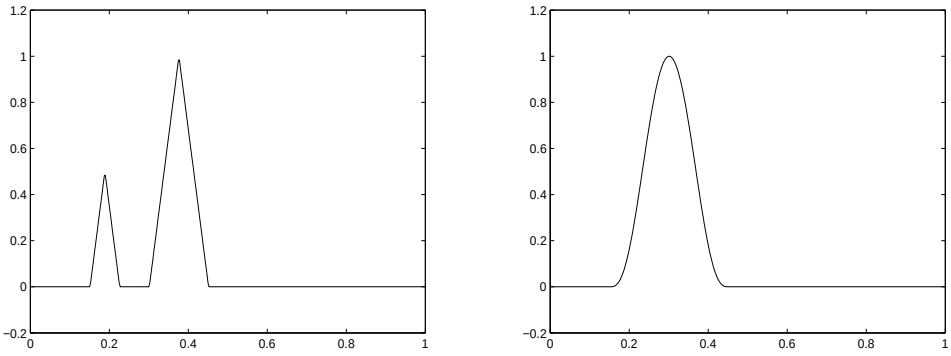

Figure 2: The testing profiles: p_1 (left) and p_2 (right).

together with the function $g(t)$ such that

$$g\big(a\cos(2\pi t), b\sin(2\pi t)\big) = \begin{cases} 1, & t \in [0.5, 0.8], \\ 0, & \text{elsewhere on } \Gamma. \end{cases}$$

A non-smooth profile p_1 and a smooth profile p_2 was tested — cf. Fig. 2, and Ref. [22] for the discretisation matrices of $\mathscr{D}$ and $\mathscr{S}$.

Our numerical calculations were carried out using Matlab. We set uniform partitions on the parameter domain [0,1] with $n = 400$ ($h = 0.0025$), and first chose $\mathbf{p}$ to obtain the solution $\mathbf{u}$ by solving $A(\mathbf{p})\mathbf{u} = S\mathbf{g}$ before generating $\mathbf{u}_0$ by adding a certain level of white noise to $\mathbf{u}(m_1+1:m_2)$ — i.e.

$$\mathbf{u}_0 = \mathbf{u}(m_1+1:m_2) + 2\delta\big[\text{rand}(m_2-m_1,1) - 0.5\big],$$

where rand denotes random numbers from the uniform distribution of the interval $(0,1)$ and δ is the noise level. We chose

$$\mathbf{p}_0 = 0.1\cdot\text{ones}(m_4-m_3,1) \in \mathbb{R}^{(m_4-m_3)}$$

as the initial guess.

4.1. Primary numerical tests on the NCP

We first investigated the relationship between the regularisation parameter, the NCP curve, and the quality of the recovered profile. We set the noise level to $\delta = 10^{-3}$ and solved the minimisation problem (2.6) with fixed regularisation parameter by the GN method proposed in Subsection 2.2. In all our tests, we adopted $m_2 - m_1 = 120$ such that the area between the ideal NCP curve and x-axis was $N_* = 30.5$. We show the results for four different cases in Figs. 3–7.

Case 1: The L_2 regularisation and $p = p_1$. We compare the recovered profiles for $\mu_1 = 10^{-4}$, $\mu_2 = 4\times10^{-5}$, $\mu_3 = 10^{-7}$ in Fig. 3. For these parameters, the corresponding areas

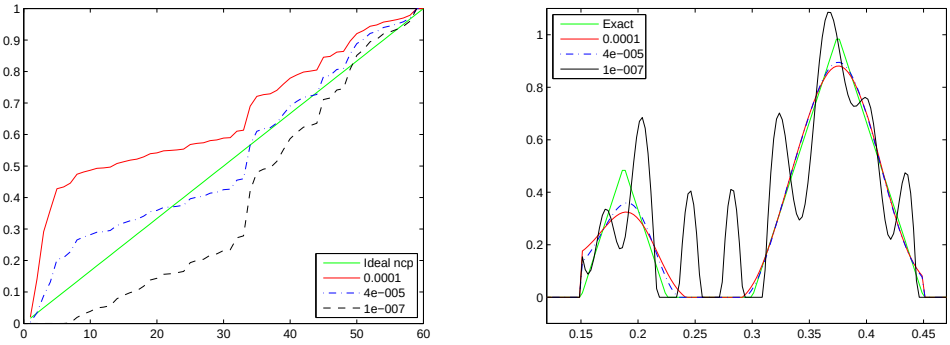

Figure 3: Regularisation parameters, NCP curves (left) and recovered profiles (right) for p_1 by using L_2 regularisation.

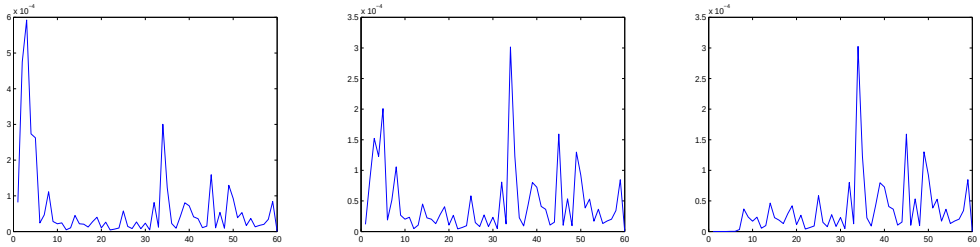

Figure 4: Curves defined by $\mathbf{e}_{\mu_1}$ (left), $\mathbf{e}_{\mu_2}$ (middle), and $\mathbf{e}_{\mu_3}$ (right).

are $N(\mu_1) = 39.43$, $N(\mu_2) = 31.95$ and $N(\mu_3) = 23.67$, respectively. The value $N(\mu_1) = N_* + 8.93$ is much larger than N_*, and from Fig. 3 it is evident that $\mathbf{r}_{\mu_1}$ is dominated by low frequency components (the first few elements of $\mathbf{e}_{\mu_1}$ are very large compared to other elements). Thus the recovered profile $\mathbf{p}_{\mu_1}$ is over smooth. The value $N(\mu_2) = N_* + 1.45$ is slightly larger than N_*, and the NCP curve C_{μ_2} is close to the ideal NCP curve. The recovered profile $\mathbf{p}_{\mu_2}$ is better than $\mathbf{p}_{\mu_1}$ in Fig. 3, so with the value $N(\mu_3) = N_* - 6.83$ considerably less than N_* we observe that $\mathbf{e}_{\mu_3}$ is dominated by high frequency components (the first few elements of $\mathbf{e}_{\mu_3}$ are very close to zero). Thus the corresponding recovered profile $\mathbf{p}_{\mu_3}$ is oscillating. We illustrate the characteristics of $\mathbf{e}_{\mu_1}$, $\mathbf{e}_{\mu_2}$ and $\mathbf{e}_{\mu_3}$ in Fig. 4.

Case 2: The L_2 regularisation and $p = p_2$. We compare the recovered profiles for $\mu_1 = 4 \times 10^{-4}$, $\mu_2 = 5 \times 10^{-5}$, $\mu_3 = 10^{-6}$ shown in Fig. 5, for which $N(\mu_1) = 54.69$, $N(\mu_2) = 30.88$ and $N(\mu_3) = 25.11$, respectively. We observe that the recovered profiles $\mathbf{p}_{\mu_1}$ and $\mathbf{p}_{\mu_2}$ are smooth and close to the original profile, which implies that a smooth profile is easy to restore and we may choose a parameter μ such that $N(\mu)$ is larger than N_*. For μ_3 we have that $N(\mu_3) = N_* - 5.39$ — i.e. $N(\mu_3)$ is considerably less than N_*. Similarly to Case 1, we deduce from Fig. 5 that $\mathbf{e}_{\mu_3}$ is dominated by high frequency components. Thus the recovered profile $\mathbf{p}_{\mu_3}$ is oscillating and not as good as $\mathbf{p}_{\mu_1}$ and $\mathbf{p}_{\mu_2}$.

Case 3: The H^1 regularisation and $p = p_1$. We compare the recovered profiles for $\mu_1 = 10^{-2}$, $\mu_2 = 10^{-3}$, $\mu_3 = 10^{-5}$ shown in Fig. 6, for which $N(\mu_1) = 38.58$, $N(\mu_2) = 29.23$

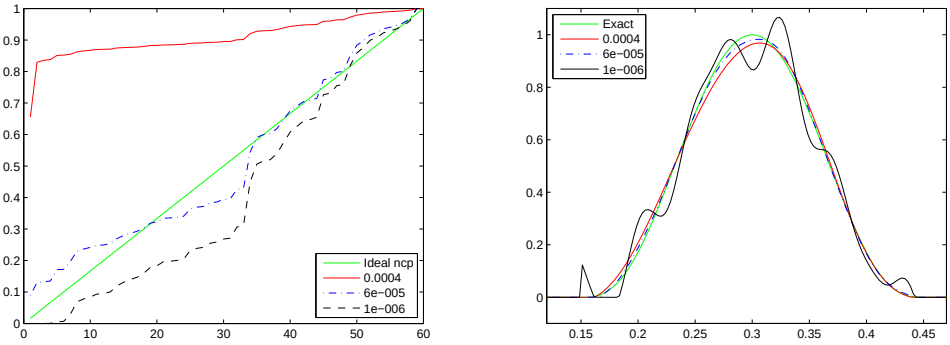

Figure 5: Regularisation parameters, NCP curves (left) and recovered profiles (right) for p_2 by using L_2 regularisation.

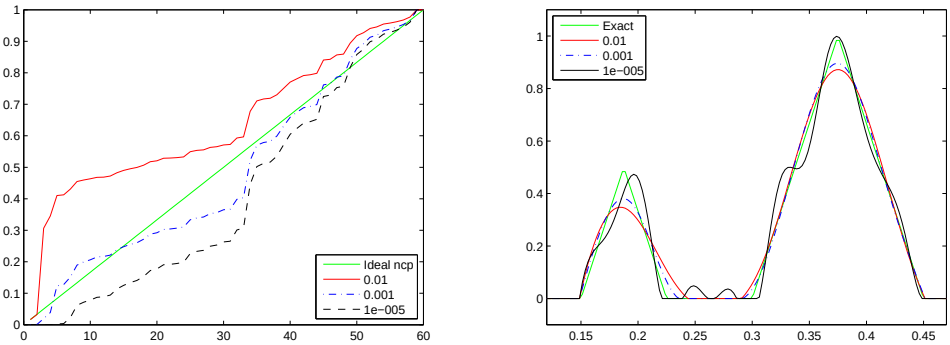

Figure 6: Regularisation parameters, NCP curves (left) and recovered profiles (right) for p_1 by using H^1 regularisation.

and $N(\mu_3) = 24.90$, respectively. For μ_1, we have $N(\mu_1) = N_* + 8.03$ — i.e. $N(\mu_1)$ is considerably larger than N_*. We observe from Fig. 6 that $\mathbf{p}_{\mu_1}$ is over smooth, but on the other hand $N(\mu_3) = N_* - 5.6$ is considerably less than N_* and $\mathbf{p}_{\mu_3}$ is oscillating. The value $N(\mu_2) = N_* - 1.27$ is close to N_*, and $\mathbf{p}_{\mu_2}$ is the best among the three recovered profiles.

Case 4: The H^1 regularisation and $p = p_2$. We compare the recovered profiles for $\mu_1 = 10^{-1}$, $\mu_2 = 2 \times 10^{-2}$, $\mu_3 = 10^{-5}$ shown in Fig. 7, for which $N(\mu_1) = 49.79$, $N(\mu_2) = 30.37$ and $N(\mu_3) = 25.10$, respectively. Similarly to Case 2, the recovered profile $\mathbf{p}_{\mu_1}$ is close to the original one despite $N(\mu_1)$ being much larger than N_*. On the other hand, $N(\mu_3) = N_* - 5.40$ is considerably smaller than N_* and $\mathbf{p}_{\mu_3}$ is oscillating. Moreover,

$$\left|N(\mu_2) - N_*\right| = \min_{i=1,2,3} \left\{|N(\mu_i) - N_*|\right\}$$

and $\mathbf{p}_{\mu_2}$ is the best among the recovered profiles.

In summary, the above results show that if the regularisation parameter μ is chosen such that $|N(\mu) - N_*|$ is small, then the NCP curve C_μ is probably close to the ideal NCP curve

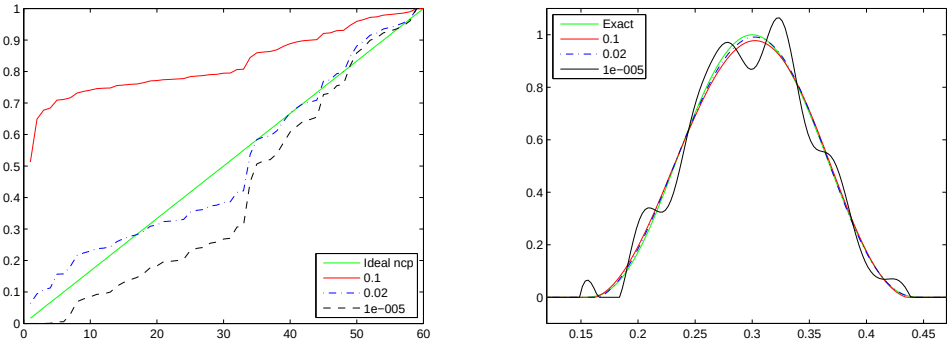

Figure 7: Regularisation parameters, NCP curves (left) and recovered profiles (right) for p_2 by using H^1 regularisation.

and the recovered profile $\mathbf{p}_\mu$ can be of satisfactory quality. On the other hand, if $|N(\mu)-N_*|$ is large then the NCP curve does not lie between the KS limits and the recovered profile may be over smooth or oscillating.

4.2. More numerical results on the NCP

Example 4.1 (Comparison of parameter selection methods)**.** We compared the performance of the NCP and L-curve methods, and also the discrepancy principle approach. The L-curve method seeks the maximum curvature point on the curve

$$\left(\log\left\|R_0A(\mathbf{p}_\mu)^{-1}\mathbf{f}-\mathbf{u}_0\right\|_2,\ \log\|W\mathbf{p}_\mu\|_2\right),$$

so we need to compute the derivatives of $\log\|R_0A(\mathbf{p}_\mu)^{-1}\mathbf{f}-\mathbf{u}_0\|_2$ and $\log\|W\mathbf{p}_\mu\|_2$ as functions of μ, which are very complicated and costly. In our numerical tests, we solved the Robin inverse problem for various μ and then computed approximate curvatures via finite differences to find the parameter corresponding to an approximate largest curvature point.

In the discrepancy principle approach, we chose the regularisation parameter μ such that the norm of residual vector equals the discrepancy in the data — i.e. we chose a μ that satisfies $\|\mathbf{r}_\mu\|_2^2=\tau\|\mathbf{e}\|_2^2$, where $\mathbf{e}$ is the noise and τ is a safety factor that we can usually set to be 1. Assuming the variation of the noise σ^2 is known, we computed the norm of the residual as $\|\mathbf{e}\|_2^2=(m_2-m_1)\sigma^2$. Here μ was searched by the secant method to obtain the root of the discrepancy principle function

$$DP(\mu)=\|\mathbf{r}_\mu\|_2^2-\tau(m_2-m_1)\sigma^2.$$

In this example, we solved the H^1 regularisation model by the GN method, and show the recovered profiles for $p=p_1$ and $p=p_2$ in Fig. 8.

Let the recovered profiles of p_i obtained by using the NCP method, the discrepancy principle, and the L-curve method be denoted by $p_{i,NCP}$, $p_{i,DP}$ and $p_{i,L}$, respectively. As seen in Fig. 8, $p_{1,NCP}$ is about the same as $p_{1,L}$ and slightly better than $p_{1,DP}$, whereas $p_{2,NCP}$ is

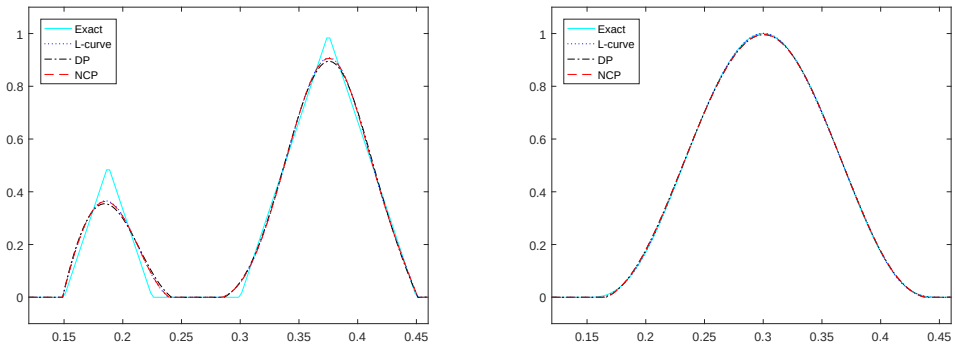

Figure 8: Recovered profiles for $p = p_1$ (left) and $p = p_2$ (right) with μ chosen by the L-curve method, the discrepancy principle method and the NCP method.

about the same as $p_{2,DP}$ and slightly less accurate than $p_{2,L}$. We note that the noise level of the measured data is required for the discrepancy principle, but not for the NCP and the L-curve methods. The drawback of the L-curve method is that it is time-consuming, since it solves the Robin inverse problem for many different μ's in order to estimate curvature values. In brief, the NCP method is more practical than both the discrepancy principle and the L-curve method. The GCV method also works in the absence of the noise level, but there is no obviously efficient algorithm when it is applied to this nonlinear problem.

For comparison, we also show the recovered profiles obtained by optimal regularisation parameters that minimise the relative error of the approximate profiles. The relative error of the approximate profile $\mathbf{p}_\mu$ is defined by

$$\mathrm{err}_\mu = \frac{\|\mathbf{p}_\mu - \mathbf{p}\|}{\|\mathbf{p}\|},$$

where $\|\cdot\|$ denotes the 2-norm and $\mathbf{p}$ is the true profile. We obtained the optimal parameter after many numerical experiments, and denote the corresponding approximate profile by $\mathbf{p}_{i,*}$, $i = 1, 2$. We see from Fig. 9 that $\mathbf{p}_{2,NCP}$ is very close to $\mathbf{p}_{2,*}$ and $\mathbf{p}_{1,NCP}$ is very close to $\mathbf{p}_{1,*}$, except at the two peaks.

Example 4.2. In this example, we applied the conjugate gradient (CG) method to solve the nonlinear least squares problem (2.6) and used the NCP method to choose a value of the regularisation parameter. Fig. 10 shows the results using the H^1 regularisation model for $p = p_1$ and $p = p_2$. We observe that the recovered profiles obtained using the CG with NCP are similar to those using the GN with NCP, but the CG method required more CPU time than the GN method — viz. 6.03 seconds in the non-smooth case and 4.24 seconds in the smooth case, whereas the GN method with NCP only took 0.57 and 0.53 seconds, respectively. In passing, we note that the regularised least squares problems can also be solved using other algorithms — e.g. Newton's method.

Example 4.3. In this example, we investigated the effectiveness of the NCP method for different levels of noise when $\delta = 10^{-2}$, 5×10^{-2} and 10^{-1}. The approximate profiles

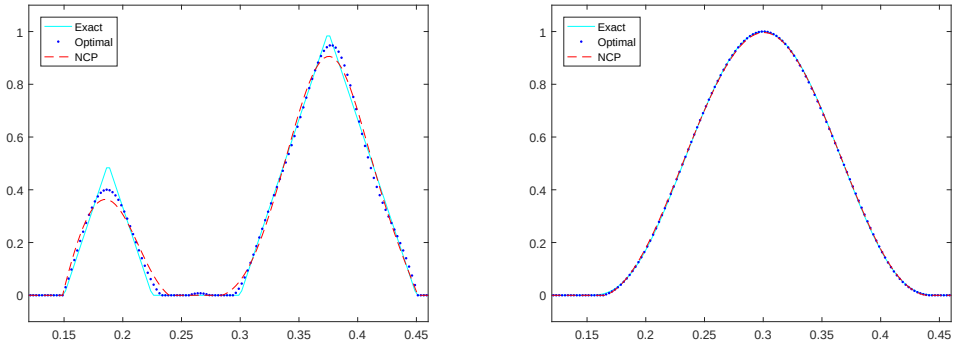

Figure 9: Recovered profiles for $p = p_1$ (left) and $p = p_2$ (right) with the optimal parameter and the one chosen by the NCP method, respectively.

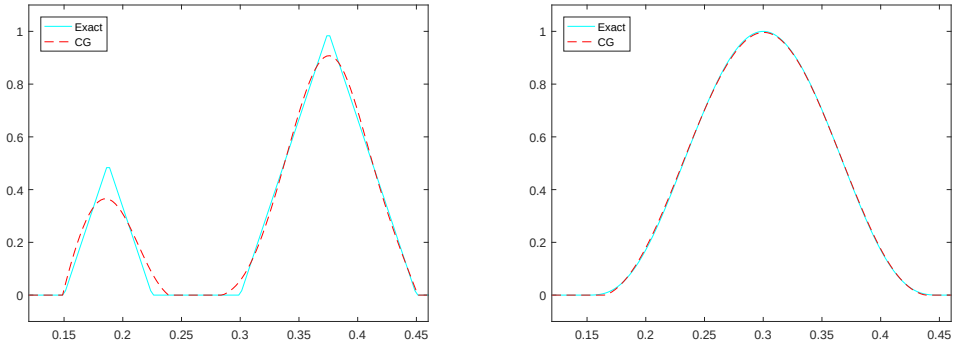

Figure 10: Recovered profiles for $p = p_1$ (left) and $p = p_2$ (right) using the CG method with NCP parameter-selection.

obtained using the H^1 regularisation with the parameter determined by the NCP method are shown in Fig. 11. The regularisation parameters determined by the NCP method as well as the optimal parameters are shown in Tables 1–4, where NL denotes the noise level, μ_* the optimal parameter, μ_{NCP} the parameter determined by the NCP method, $\text{err}_* = \text{err}_{\mu_*}$ and $\text{err}_{NCP} = \text{err}_{\mu_{NCP}}$. We observe that in some cases the difference between μ_{NCP} and μ_* is significant, while that between the relative errors is small (especially for the smooth profile $p = p_2$) — cf. the numbers underlined. In brief, although the NCP method cannot seek out the optimal parameter, reliable results are obtained.

5. Concluding Remarks

We have proposed a regularisation parameter choice method for the Robin inverse problem using the normalised cumulative periodogram (NCP) curve of the residual vector. Numerical examples show that the proposed method is very effective. The main idea of the

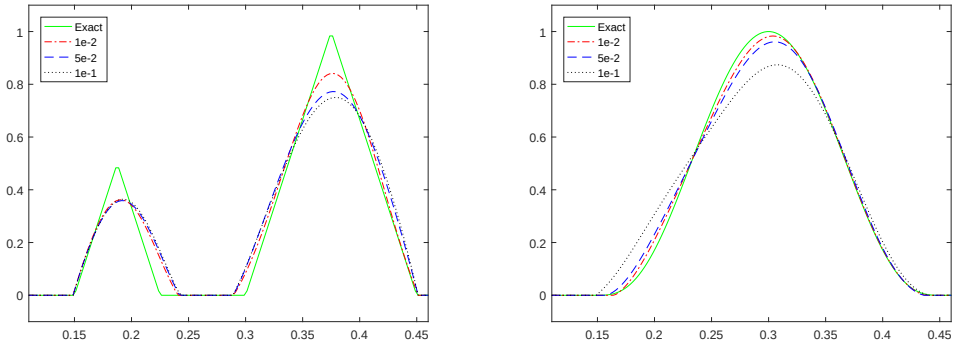

Figure 11: Recovered profiles for $p = p_1$ (left) and $p = p_2$ (right) using the CG method with NCP parameter-selection.

Table 1: Parameters chosen and relative errors of recovered profiles with H^1 regularisation for $p = p_1$.

NL	μ_{NCP}	μ_*	$\frac{\lvert\mu_{NCP}-\mu_*\rvert}{\mu_*}$	err_{NCP}	err_*	$\frac{\mathrm{err}_{NCP}-\mathrm{err}_*}{\mathrm{err}_*}$
1e–2	3.4776e–2	1.1512e–2	2.0208	1.2356e–1	1.1211e–1	1.0213e-1
5e–2	2.6870e–1	2.6602e–1	1.0074e–2	1.7252e–1	1.7238e–1	8.1216e–4
1e–1	5.1968e–1	5.1448e–1	1.0107e-2	1.9090e–1	1.9072e–1	9.4379e–4

Table 2: Parameters chosen and relative errors of recovered profiles with H^1 regularisation for $p = p_2$.

NL	μ_{NCP}	μ_*	$\frac{\lvert\mu_{NCP}-\mu_*\rvert}{\mu_*}$	err_{NCP}	err_*	$\frac{\mathrm{err}_{NCP}-\mathrm{err}_*}{\mathrm{err}_*}$
1e–2	7.8272e–2	6.5319e–2	1.9830e–1	3.2814e–2	3.2464e–2	1.0781e–2
5e–2	3.8051e–1	1.8454e–1	1.0619	8.9501e–2	8.0973e–2	1.0532e–1
1e–1	8.9224e–1	3.3659e–1	1.6508	1.4158e–1	1.2733e–1	1.1191e–1

Table 3: Parameters chosen and relative errors of recovered profiles with L_2 regularisation for $p = p_1$.

NL	μ_{NCP}	μ_*	$\frac{\lvert\mu_{NCP}-\mu_*\rvert}{\mu_*}$	err_{NCP}	err_*	$\frac{\mathrm{err}_{NCP}-\mathrm{err}_*}{\mathrm{err}_*}$
1e–2	3.1023e–4	2.0137e–4	5.4059e–1	1.2140e–1	1.1422e–1	5.9166e–2
5e–2	1.724e–3	1.6897e–3	2.0304e–2	2.0656e–1	2.0602e–1	2.5850e–3
1e–1	3.4844e–3	3.4495e–3	1.0101e–2	2.6017e–1	2.5987e–1	1.1694e–3

Table 4: Parameters chosen and relative errors of recovered profiles with L_2 regularisation for $p = p_2$.

NL	μ_{NCP}	μ_*	$\frac{\lvert\mu_{NCP}-\mu_*\rvert}{\mu_*}$	err_{NCP}	err_*	$\frac{\mathrm{err}_{NCP}-\mathrm{err}_*}{\mathrm{err}_*}$
1e–2	3.3342e–4	5.8209e–4	4.2720e–1	7.6307e–2	7.3751e–2	3.3503e–2
5e–2	1.3268e–3	1.6351e–3	1.8857e–1	1.5364e–1	1.5249e–1	7.4270e–2
1e–1	2.6243e–3	2.5463e–3	3.0610e–2	2.0961e–1	2.0958e–1	1.0229e–4

NCP method is to choose a suitable value of the regularisation parameter such that the corresponding residual vector is a nearly white noise. Obviously, this idea can be used in other models for selecting a suitable regularisation parameter.

Acknowledgments

We thank the anonymous referees for providing valuable comments and suggestions. This work was supported by the National Natural Science Foundation of China Grant No. 11271238.

References

[1] G. Alessandrini, L.D. Piero and L. Rondi, *Stable determination of corrosion by a single electrostatic boundary measurement*, Inverse Problems **19**, 973-984 (2003).
[2] F. Cakoni and R. Kress, *Integral equations for inverse problems in corrosion detection from partial Cauchy data*, Inverse Problems and Imaging **1**, 229-245 (2007).
[3] S. Chaabane, C. Elhechmi and M. Jaoua, *A stable recovery method for the Robin inverse problem*, Math. Comput. Simul. **66**, 367-383 (2004).
[4] S. Chaabane, I. Feki and N. Mars, *Numerical reconstruction of a piecewise constant Robin parameter in the two- or three-dimensional case*, Inverse Problems **28** 065016, 19pp (2012).
[5] S. Chaabane, I. Fellah, M. Jaoua and J. Leblond, *Logarithmic stability estimates for a Robin coefficient in two-dimensional Laplace inverse problems*, Inverse Problems **20**, 47-59 (2004).
[6] S. Chaabane and M. Jaoua, *Identification of Robin coefficients by the means of boundary measurements*, Inverse Problems **15**, 1425-1438 (1999).
[7] D. Chen, S. Maclachlan and M. Kilmer, *Iterative parameter-choice and multigrid methods for anisotropic diffusion denoising*, SIAM J. Sci. Comput. **33**, 2972-2994 (2011).
[8] M. Choulli, *On the determination of an unknown boundary function in a parabolic equation*, Inverse Problems **15**, 659-667 (1999).
[9] J. Dennis and R. Schnabel, *Numerical Methods for Unconstrained Optimisation and Nonlinear Equations*, SIAM (1996).
[10] W. Fang and S. Zeng, *A direct solution of the Robin inverse problem*, J. Integral Equ. Appl. **21**, 545-557 (2009).
[11] D. Fasino and G. Inglese, *An inverse Robin problem for Laplace's equation: Theoretical results and numerical methods*, Inverse Problems **15**, 41-48 (1999).
[12] D. Fasino and D. Inglese, *Discrete methods in the study of an inverse problem for Laplace's equation*, SIAM J. Numer. Anal. **19**, 105-118 (1999).
[13] G.H. Golub, M. Heath and G. Wahba, *Generalised cross-validation as a method for choosing a good ridge parameter*, Technometrics **21**, 215-223 (1979).
[14] P.C. Hansen, M.E. Kilmer and R.H. Kjeldsen, *Exploiting residual information in the parameter choice for discrete ill-posed problems*, BIT. **46**, 41-59 (2006).
[15] P.C. Hansen and D.P. O'leary, *The use of the L-curve in the regularisation of discrete ill-posed problems*, SIAM J. Sci. Comput. **14**, 1487-1503 (1993).
[16] G. Inglese, *An inverse problem in corrosion detection*, Inverse Problems **13**, 977-994 (1997).
[17] B. Jin, *Conjugate gradient method for the Robin inverse problem associated with the Laplace equation*, Int. J. Numer. Meth. Eng. **71**, 433-453 (2007).
[18] B. Jin and P. Maass, *Sparsity regularisation for parameter identification problems*, Inverse Problems **28** (2012) 123001–123071.

[19] B. Jin and J. Zou, *Inversion of Robin coefficient by a spectral stochastic finite element approach*, J. Comp. Phys. **227**, 3282-3306 (2008).
[20] B. Jin and J. Zou, *Numerical estimation of piecewise constant Robin coefficient*, SIAM J. Control Optim. **48**, 1977-2002 (2009).
[21] R. Kress, *Linear Integral Equations*, 2nd edition, Springer, New York (1999).
[22] F. Lin and W. Fang, *A linear integral equation approach to the Robin inverse problem*, Inverse Problems **21**, 1757-1772 (2005).
[23] Y. Ma and F. Lin, *Conjugate gradient method for estimation of Robin coefficients*, East Asian J. Appl. Math. **4**, 189-204 (2014).
[24] P. Mojabi and J. LoVetri, *Adapting the normalised cumulative periodogram parameter-choice method to the Tikhonov regularisation of 2-D/TM electromagnetic inverse scattering using born iterative method*, Prog. Electromagn. Res. M **1**, 111-138 (2008).
[25] V.A. Morozov, Z. Nashed and A.B. Aries, *Methods for Solving Incorrectly Posed Problems*, Springer, New York (1984).
[26] B.W. Rust and D.P. O'Leary, *Residual periodograms for choosing regularisation parameters for ill-posed problems*, Inverse Problems **24**, 34005-34034 (2008).